Geoelectrical Characterization of Sulphate Rocks

Ander Guinea Maysounave

Programa de Doctorat de Ciències de la Terra

GEOELECTRICAL CHARACTERIZATION OF SULPHATE ROCKS

Ander Guinea Maysounave

2011

Advisors / Directors de tesi:

Drs. Elisabet Playà Pous & Lluís Rivero Marginedas

Departament de Geoquímica, Petrologia i Prospecció Geològica

UNIVERSITAT DE BARCELONA

Application examples

Ander Guinea 2011

6

.1 GYPSUM DEPOSIT IN PIRA (TARRAGONA)

.1.1 Introduction

The exploitability of a gypsum deposit area has been studied in order to classify the different gypsum types (with the geoelectrical classification of gypsum rocks) present and identify the volume of the profitable rock. In this area, IP measures have been successfully recorded displaying polarization trends in relation with the terrain distribution. A 3D section has been elaborated from parallel 2D acquisition, displaying the resistivity distribution of the terrain horizontal sections additionally to the vertical ones.

.1.2 Materials and methods

Eight ERT profiles were performed in the studied gypsum formation (figure 6.1), located close to the Pira village (Tarragona, NE Spain). The disposition of the profiles was parallel and E-W orientated, with the exception of two oblique profiles.

There are lots of different arrays used in the electrical prospection methods (Szalai and Szarka 2008) with different depth of investigation and vertical resolution values (Szalai et al. 2009). In this survey some of the most used arrays for ERT were tried (Dipole-Dipole, Wenner

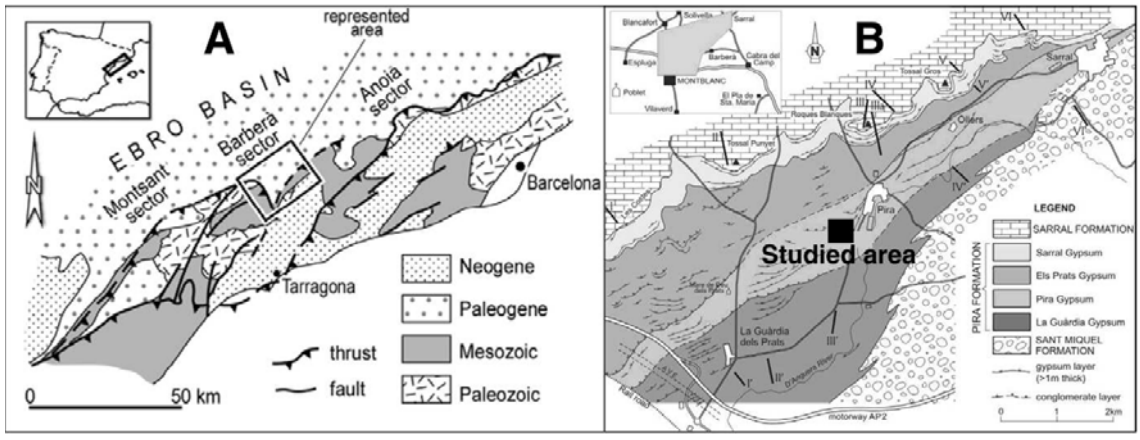

Figure 6.1: A) Geological location of the Barberà sector in the SE margin of the Ebro Basin (NE Spain). B) Geological map of the Eocene evaporite units composing the Pira Fm. (modified from Ortí et al. 2007). The black square indicates the studied area.

alpha and Wenner-Schlumberger) showing similar results. Finally Wenner-Schlumberger was selected given that the unit dips less than 15ºNNW and displayed apparent lateral continuity. The measures of apparent electrical resistivity were performed with a SYSCAL PRO switch with 48 electrodes separated by 2 meters between them with internal power supply. In 3 of these ERT profiles, IP in time domain measures were acquired with arithmetic configuration for 500 ms time lapse (Dahlin 2002). On the purpose of processing data, RES2DINV program was used to carry out the inversion. This program uses the smoothness-constrained least-squares method (deGroot-Hedlin and Constable 1990; Sasaki 1992) in his inversion routine.

An additional 15 meters continuous coring drill was done in the plot to support the imaging prospection campaign (figure 6.2). The cores were accurately petrographically described and sampled. The amount of non-gypsum minerals was quantified by dissolving of about 0.5 g of 6 powdered gypsum samples in 250 mL of distilled water (solubility of gypsum is about 2.4 g/l); solutions were shook during 24 hours and subsequently filtered. The remnant after filtering corresponds to the non-soluble impurities of the gypsum rock. The results of these laboratory essays are not absolutely representative of the whole deposit due to the lixiviation of finest materials (lutites) during the water-mediated drilling works. The residual material was mineralogically characterized by X-ray diffraction (XDR). In addition, representative thin sections of the whole deposit have been studied under standard petrographic microscope.

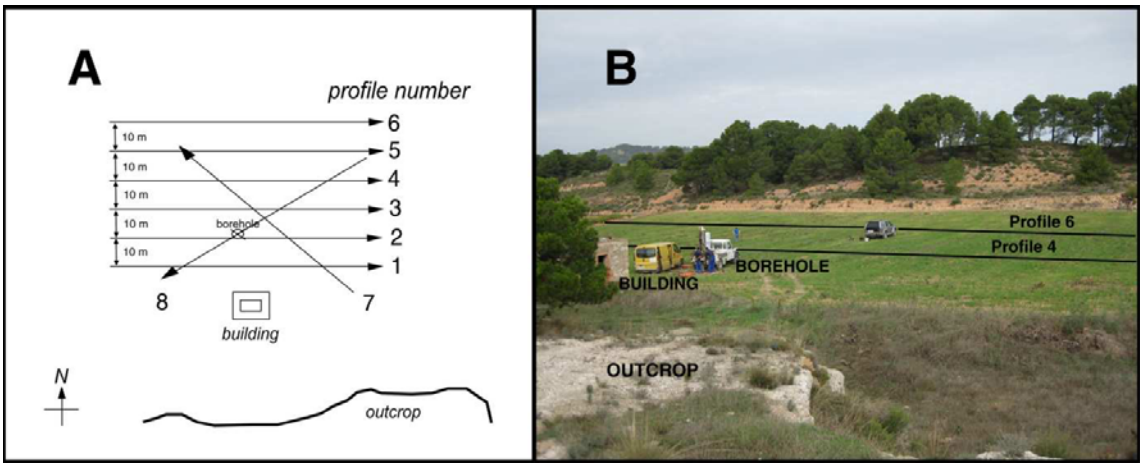

Figure 6.2: A) Sketch and B) photograph of the performed imaging profiles (1-8) and location of the Pira borehole in the studied plot (Pira Village, Tarragona, NE Spain). General location of the studied plot of land in figure 6.1.

.1.3 Geological setting

During the Paleogene, an evaporitic lacustrine sedimentation episode took place along the SE of Catalan margin of the Tertiary Ebro Basin (Ortí 1990; Ortí et al. 2007). The Conca de Barberà sector (where the study is situated) is a depression excavated on the Eocene and Oligocene materials of the Ebro basin (figure 6.1A). In the Catalan margin the sedimentation was bound to the tectonic evolution of the Catalan Coastal Range. During the Paleogene compression NNW verging structures as folds and thrusts developed in the area. These structures were related to pre-existing basement faults. In the Miocene, these structures acted as normal faults during an extensional episode (Anadón et al. 1985; Cabrera et al. 2004).

The studied materials correspond to the Pira Gypsum of the Pira member, belonging to the Montblanc formation. They are characterized by secondary gypsum in surface (coming from hydration of anhydrite) and anhydrite at depth. At some levels, the gypsum appears in centimetric nodules (sometimes up to metric sized nodules) or enterolithic layers. These structures are inherited from anhydrite (Ortí et al. 2010). Several gypsum units, with individual thicknesses ranging from 50 to 100 m, are intercalated within various detritic units.

The studied units can be separated into two different terms. The lower term is constituded of red lutites with few intercalations of sandstones. The upper term is less terrigenous than the lower one and corresponds to the evaporite sequence. Additionally, there are lateral variations in the composition of gypsum deposits related with depositional processes. Depending on the position of the gypsum precipitation within the lacustrine basin, the quantity of lutite in the gypsum rock is low (offshore) or high (near the shore). This is due to the proximity of terrigen contribution.

The plot of land where the profiles and the well were performed is located near to the Pira village (figure 6.1B). The outcropping gypsum layers (at the southern part of the terrain) are expected to be represented in the ERT image.

.1.4 Results

A total of 8 electrical resistivity profiles were carried out in the studied area. In the performed ERT profiles the root mean square (RMS) error between the measured and calculated values was low (<5%). Two types of materials are observed in all the images: a)

materials with low electrical resistivity values (1-50 ohm.m), blue in colour; and, b) materials with high electrical resistivity values (>900 ohm.m), displaying red-purple colours (figure 6.3). The intermediate values are assigned to the transition between these two types of materials, which depend in turn to the depth. Given that the resolution decreasing with depth, these boundaries are well defined in the ERT lines when they are shallow, and diffuse when they are at the lower part of the profile (as in figure 6.3E).

The real electrical resistivity profiles 1 and 2 (figure 6.3, A and B) show a surface layer (up to 1-2 meters depth) composed of low electrical resistivity materials (~10 ohm.m); these level are overlaying a high electrical resistivity material body (800-1000 ohm.m). Underneath this resistive body, resistivity decreasing materials are recorded from a depth of 7 meters (~800 ohm.m) to 12 meters (<100 ohm.m). In the profiles 4 and 5 (figure 6.3D and E), the resistive body is thicker and continue at depth. The deeper low electrical resistivity materials do not appear in these profiles. The boundary between the superficial layer and the resistive body is slightly tilted towards north, as clearly reflected in the profiles 7 and 8 (figure 6.3G and H), thus making thicker the uppermost low resistive body from the profile 1 to 6. In the profile number 6 (figure 6.3F) which is the northern one, this boundary is not cut by the ERT. In order to get better view of the deposit, 3D resistivity model of the studied area has been carried out by interpolation of the inverted resistivity data. This model is displayed as horizontal slices at different depths in the figure 6.4. It can be seen a trend of high resistivity values moving towards north while the depth increases.

The chargeability of the terrain was measured in the profiles 2, 7 and 8. The IP anomalies (until 6 mV/V) have a trend in accordance with the resistivity decreasing materials in the ERT profiles (figure 6.5A, B and C; figure 6.6), indicating a lithologic control. The match between the trend of IP values and the lithologic composition is especially good in the case of profile 2 which is parallel to the stratification. In the case of profiles 7 and 8, which are oblique to the structure, the boundary between gypsum impure layers and the lutite layers is undefined in the IP imaging. All the profiles show a surface layer with background values (1.5-2.5 mV/V), which match with the low electrical resistivity surface values from A unit (figure 6.6), and a depth-increasing anomaly, up to 6 mV/V. In the profile 2 this anomaly decreases below 12 meters.

Detailed petrological study of the Pira cores from the Pira well has permitted to distinguish several subunits in the gypsum layer, according to the gypsum lithofacies and the amount of accompanying minerals. Studied gypsum layer is mainly constituded of

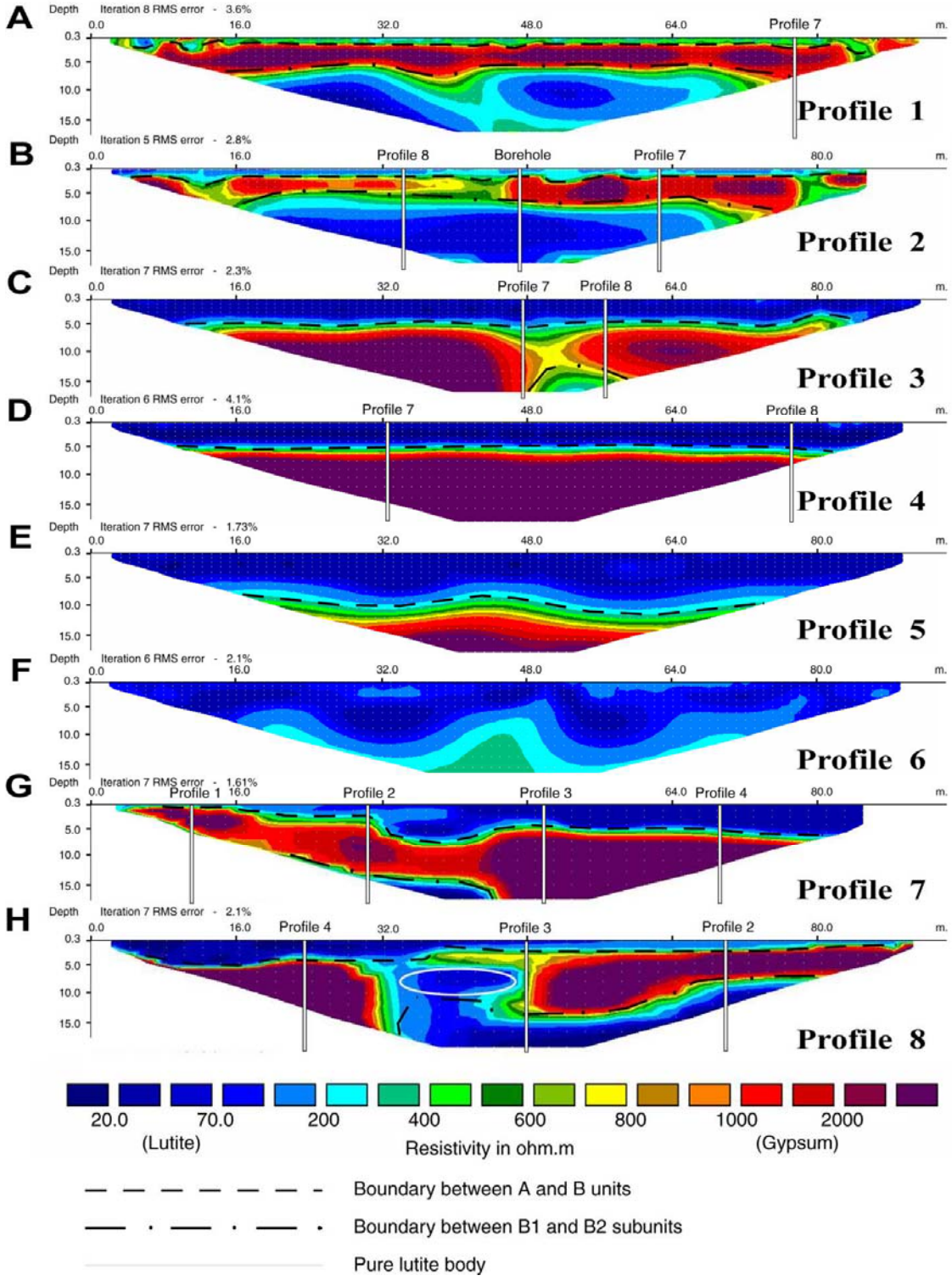

Figure 6.3: Electrical imaging profiles (Pira village, Ebro Basin, NE Spain). Location of the profiles in figures 6.1 and 6.2. The profiles show the points where they are cut by other profiles and the situation of the borehole.

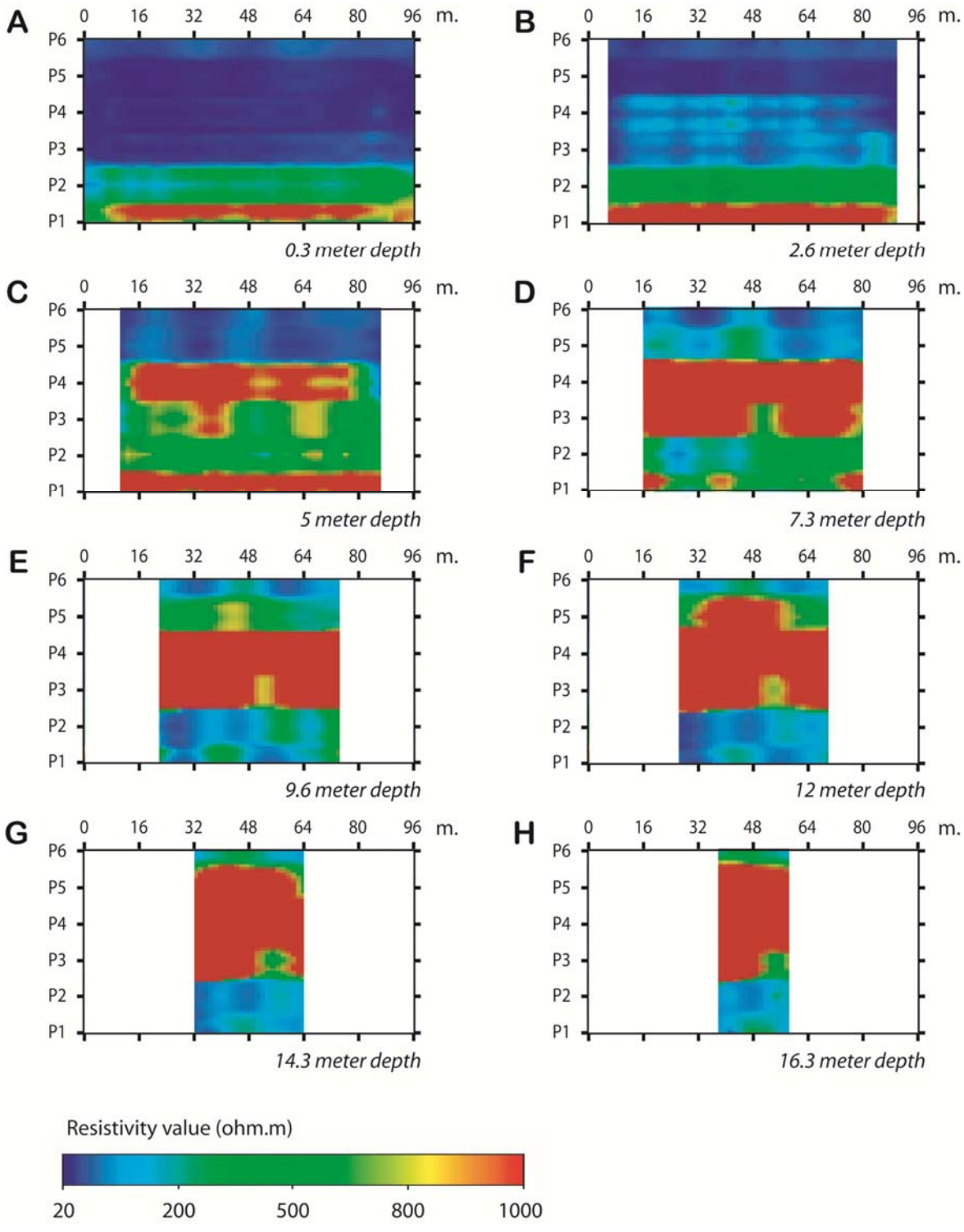

Figure 6.4: Horizontal slices at different depth of the studied area showing the electrical resistivity values. The slices have been elaborated from the interpolation of the ERT profiles in figure 6.3. The location of the profiles is marked with P and his corresponding number in the Y axis of each slice.

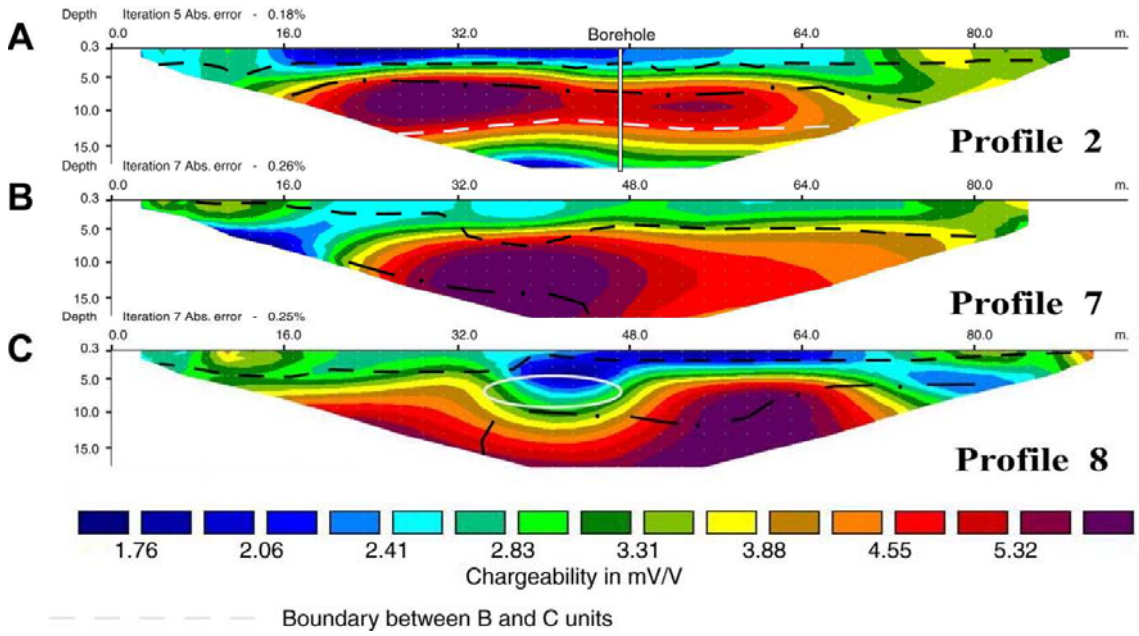

Figure 6.5: Electrical chargeability profiles (Pira village, Ebro Basin, NE Spain). Location of the profiles in figures 6.1 and 6.2. The B-C boundary is interpreted from the IP measuring.

microcrystalline massive gypsum (with traces of anhydrite within) with diffuse bedding and lamination (figure 6.7). Noduls of microcrystalline (alabastrine) pure gypsum and chert and patches of carbonates are frequent. Reddish and brownish colours in gypsum are due to the irregular presence of enclosing clays and carbonates (calcite and dolomite) within the gypsum matrix, respectively. The purity of the gypsum rock is from 56.3% to 93.9% (figure 6.6), and colouring from white to red-brown is directly related to the increase of enclosing minerals.

The residue from the essays (formed by the non-evaporitic phases) is constituted by clay minerals, carbonates (calcite and dolomite), quartz and celestite. Regarding the percentages obtained in the purity analyse, it must be noted that the drilling process was water-mediated, which solved little quantity of gypsum at the first meters of the drilling (the fluid that left from the borehole was white in colour). The cores recovered below a depth of 6.8 meters were smaller and fractured and the water used in the perforation became brownish (because of clay leaching). This suggests that important amount of clay minerals were leached and therefore the real purity of gypsum would be even lower than the measured in the analysis.

1.5 Discussion

The target of the study is a gypsum layer, overlayed by lutites, which was exploited in the XX century. The 5 uppermost meters of the unit outcrop in the walls of the old quarries. Three different units have been described in the imaging profiles. They are interpreted as (from top to bottom): a) a lutite surface soil, b) a gypsum layer, and c) a basal gypsum bearing lutite unit, which is only present in the profiles 1 and 2 (figure 6.3A and B). The real resistivity sections display a disposition sinking toward to the north; this dipping can be measured at the southern outcrop.

The uppermost gypsum-lutite boundary is well defined in the tomographyc profiles, due to the high resistivity contrast between lutites and gypsum (around 10 ohm.m for the lutites and higher than 800 ohm.m for the gypsum rocks). The calculated values for gypsum at some ERT profiles (>2000 ohm.m) are higher than the values given for pure gypsum. This is due to the difficulties of the electric current to pass through the resistive levels; on these gypsum levels the sensitivity of the method in data acquisition decreases, giving anomalous values. Nevertheless, even the values are not totally realistic the general structure is well defined. The electrical resistivity slices show that the boundaries are neat and E-W oriented (figure 6.4). The slices display the layer of the evaporitical deposit sinking towards north at depth represented by the high resistivity values.

In the log description, the gypsum unit is divided into (figure 6.6): 1) upper B1 subunit, from 0.9 to 6.8 m depth, made of pure (purity up to 94%), massive and white to brownish secondary microcrystalline gypsum and 2) lower B2 subunit, from 6.8 to 11.8 m depth, formed by massive to laminated reddish secondary microcrystalline gypsum with abundant red lutites (purity of gypsum from 56 to 91%). The B2 subunit can be separated into 2 additional terms in relation to his composition: a) where the composition is very lutitic (around 50%) and b), whose purity decreased with depth starting from a pure composition (around 90%). The samples from outcrop which purity has been analysed would correspond to the first 5 meters of the B1 subunit.

The purity obtained in these samples (99% and 91%) matches with the purity obtained on core samples at those depths (92.2% and 93.9%). The change of composition in the gypsum rocks has a sedimentary origin. Lateral variations (in composition and thickness) are current in evaporite rocks. The evaporite deposits can be very heterogeneous because his precipitation is usually bonded to irregular input of detritical particles.

Comparison of the composition (% of gypsum) of the samples from the cores with the resistivity values obtained in the profile 2 (figure 6.6) evidences that the uppermost lutite-gypsum boundary is abrupt and well defined. The resistivity values of lutites are lower than 20 ohm.m and values of 800 ohm.m are rapidly achieved at 0.9 m depth. This boundary surface

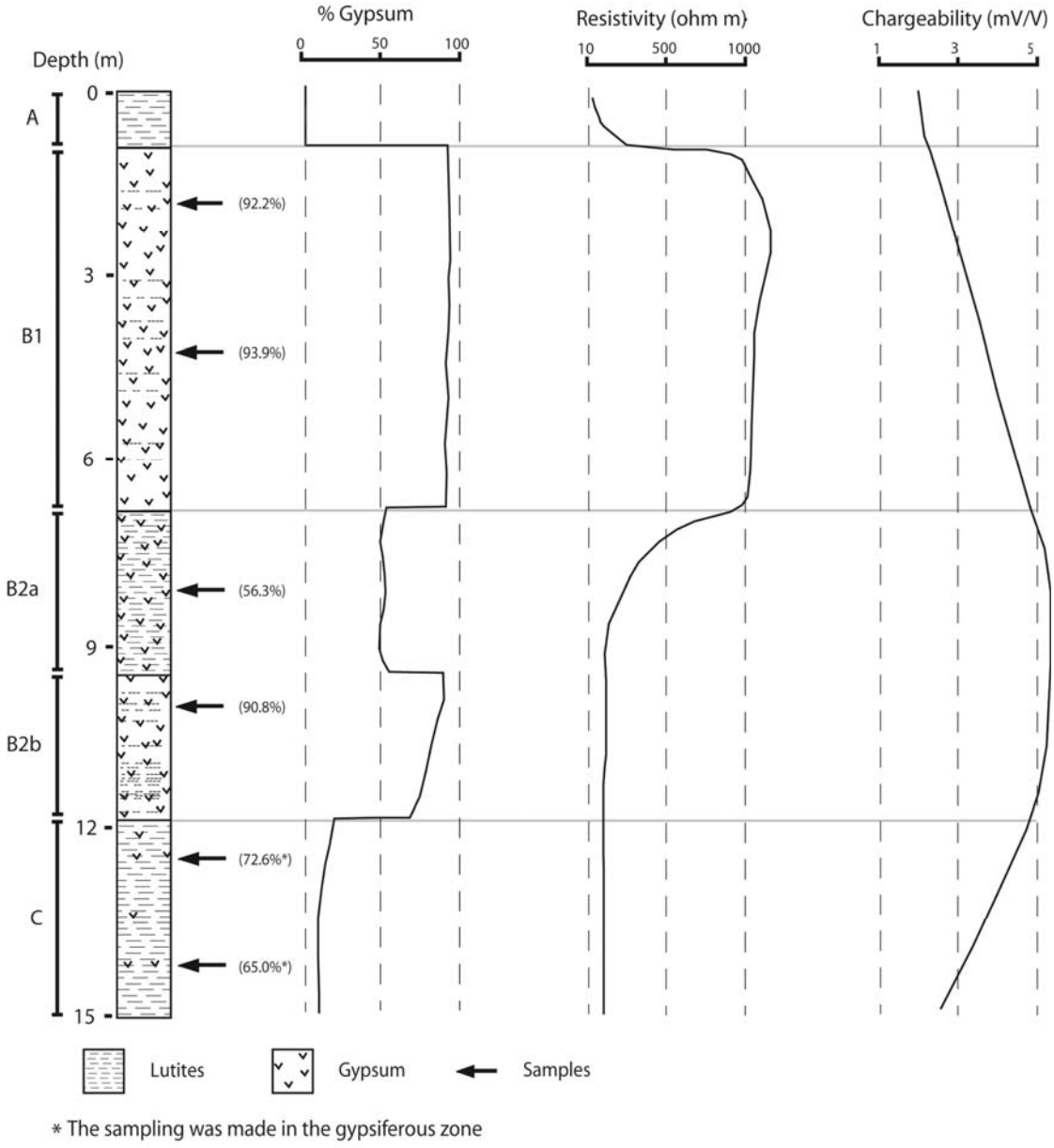

Figure 6.6: Simplified log of the Pira well (Ebro Basin), and relationships between the purity of the gypsum rocks and their geoelectrical response. Values in brackets indicate the percentage of gypsum in the analysed samples. The % gypsum curve is extrapolated from the sampling; the resistivity and the chargeability curves are taken from the values displayed in the profile 2 from figures 6.3A and B.

(boundary between A and B units) is clearly recorded in the profiles 1 to 8, which depth at each profile is in accordance with the NNW dipping of the layers. Conversely, the lowermost gypsum-lutite boundary (boundary between B and C units) is progressive and diffuse in the tomographyc profiles 1 and 2; the resistivity values decrease from 800 ohm.m, at 6.8 m depth (which represent the boundary between B1 and B2 subunits), to 100 ohm.m, at 12 m depth. Thus, geological interpretation of the ERT profile could be confuse and uncertain, while the boundary between B and C units is clearly recognised at 11.8 m depth in the Pira well.

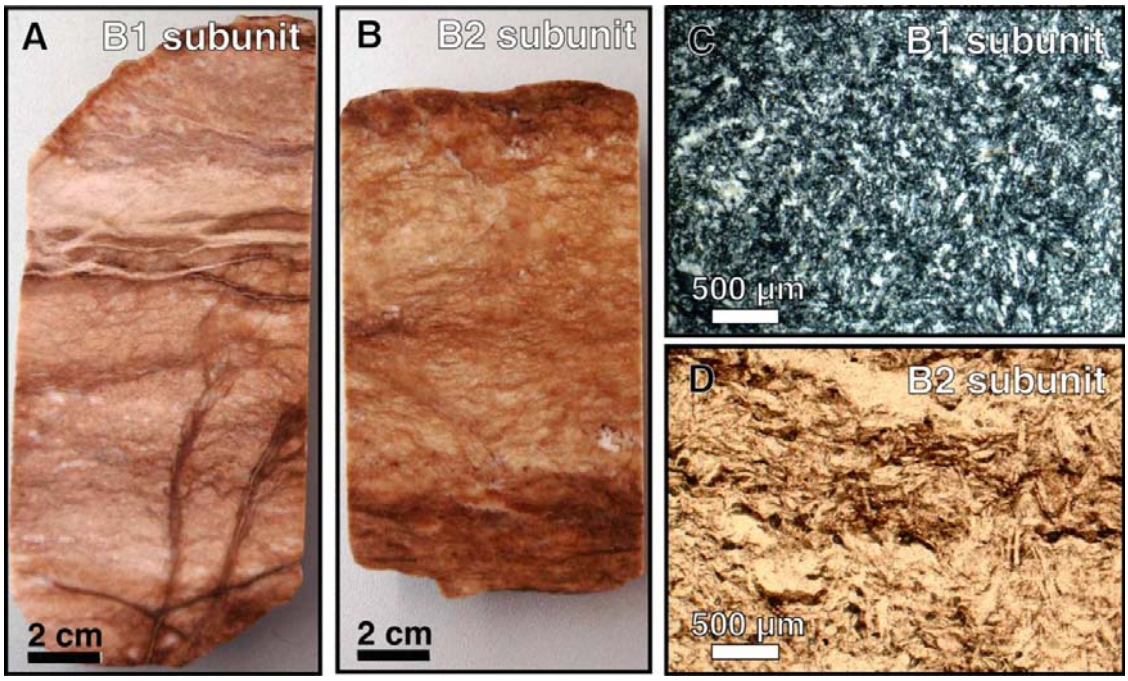

Figure 6.7: A) Hand sample of the Pira core from the B1 subunit. Even the brownish colouring of the core, which is due to the disperse presence of calcite, the main constituent is gypsum (>90%). B) Hand sample of the Pira core from B2b subunit. The reddish colouring is due to the presence of clay-rich laminae. C) Photomicrograph (cross polarized light) of the gypsum rock from B1 subunit with alabastrine texture (microcrystalline pure gypsum). D) Photomicrograph (plane polarized light) of the non-pure gypsum rock from the B2a, showing diffuse clay-rich laminae within the host-gypsum rock. Pseudomorphs of anhydrite crystals (prisms), replaced by gypsum, are evidenced.

With the information obtained from the core is evidenced that the progressive decreasing of resistivity in 1 and 2 ERT profiles is due to B2 subunit presence. This phenomenon is related to a decreasing of gypsum purity in the whole-rock. However, it is not possible to distinguish between B2a and B2b terms in the ERT lines because of the resolution of the method (Sumanovac and Domininkovic 2007). The value of electrical resistivity becomes

stable at 12 meters depth, with a value of 20 ohm.m; this reflects the boundary between B and C units. The C unit contains minor quantity of dispersed gypsum, which slightly increases the value of resistivity with respect to these of the lutites (<10 ohm.m).

The highest resistivity values in the profile 2 correspond to the purest gypsum level (B1 subunit). Conversely, the highest chargeability values are registered in the B2 subunit, which is richer in lutites than the previous one. Additionally, the boundary between B and C units (found at 12 meters in the borehole), which is not shown at the electrical imaging, matches with the chargeability decreasing in the profile 2. This boundary is interpreted in the figure 6.5A. The increasing of the chargeability values can be explained as an electrical condenser effect produced by the alternation of thin clay laminae and gypsum thin laminae, where gypsum would act as a dielectric material. There is another possible explanation based on the dispersion and absorption of electrical currents in dielectric materials. Cole and Cole (1941) defined the parameters for molecular scale polarisation interactions in scattered ions. At macroscopic scale, the Cole-Cole parameters have been resolved from chargeability values given by metallic mineral particles in a rather poorly conducting matrix (Efferso 2006).

The most plausible lithological interpretation of the studied area is displayed in the figure 6.8, on the basis of the geoelectrical response of the materials (both resistivity and chargeability) and the stratigraphical and petrological studies. This model corresponds with the evaporitical structure in the situation of profile 8, which is representative of the whole evaporitic deposit. All the boundaries between units are sedimentary in origin, showing common lateral and vertical compositional changes. The horizontal variation of purity between B1 and B2 unities is interpreted as a transition. Towards north, the thickness of gypsum body increases. The centre of the evaporitical basin would be in the same direction. However the southern part would receive the influence of terrigen contribution, which is represent by B2 unit. The electrical resistivity imaging has allowed defining the body of pure gypsum and his change of purity. In the profile 8 is also displayed a lutite body without gypsum within. This body would be explained as local little mound when the deposition took place. Another possible explanation is synsedimentary dissolution created by a water current channel with following lutite infilling. There are no evidences of large dissolution in this area but there is also the possibility of recent local-scale dissolution. The body is located in a less resistive area which is related to the presence of more lutite, this is shown in the centre part of the slice at 5 meter depth (figure 6.4C).

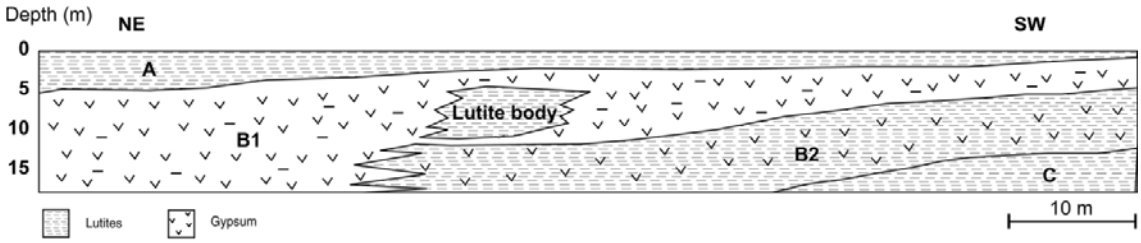

Figure 6.8: Interpretative model based on the ERT and IP images from the profile 8 (location in figure 6.2). The different units A, B and C of the log (defined in figure 6.6) are displayed together with the lutite body.

From the point of view of the geoelectrical classification of gypsum rocks, the unit B is classified as Pure Gypsum; this would be the economically profitable layer of the deposit. B2 unit corresponds to Transitional (Dirty) Gypsum and C to gypsum bearing Lutites. So this area displays the 3 different types of gypsum rocks.

The fact of having a 3D structure could have affected the measurements (Nyári and Kamli 2007), but in this case the lateral changes are not abrupt and the ERT profile images are coherent between them (profiles 1 to 6 respect 7 and 8, which are oblique). In the case of chargeability measurement, it has permitted to interpret the lutite inclusion in addition to distinguish between impure gypsum and pure lutite.

.2 GYPSUM PURITY SURVEY IN AN ACTIVE QUARRY

.2.1 Introduction

Besides the presence of anhydrite, which has been previously explained in chapter 4.2; the continuity in the purity of the deposit is the most important factor while quarrying gypsum bodies. When the extracted material is treated, no changes in the mean purity make the processing easier and cheaper. Thus, a good knowledge of the purity variations of the gypsum under exploitation allows improving the extraction planning. The current used method in quarries in order to estimate the purity of the extracted material consists on boreholes and taking samples directly from the quarry front. Generally, these samples are powdered, dried at a T<50ºC and dehydrated at 400 ºC. The weight difference between the initial and final sample indicates the water loss and therefore the quantity of gypsum. This method is known as the "combined water content test" (UNE 102032 regulation).

With ERT is possible to obtain an estimation of the purity changes in the quarry front, giving a general view of the main variations. With this information the extraction of the gypsum mineral can be optimized at immediate and future stages of the exploitation. In any case, this method is proposed as complementary to the currently used methods for the estimation of the deposit purity; which also are useful for the characterization.

.2.2 Materials and methods

Five ERT profiles have been performed in an active gypsum quarry of the studied evaporitic formation (figure 6.9), located close to the village of Gelsa (Zaragoza, N Spain). This quarry has been active in the last years extracting up to $9x10^5$ tones of unprocessed gypsum per year (the production is approximately the 55% of the extracted mineral) and it is still active. The ERT lines have been spread parallel to the quarry fronts currently under exploitation (figure 6.10) with the exception of profile 1; which has been located in a zone of future expansion of the quarry.

The used resistivimeter was a SYSCAL PRO switch with 48 electrodes with an electrode spacing of 2 meters with external power supply. As the terrain was not suitable because of the high porosity and dryness of the ground in which the electrodes were nailed, water was poured in the base of the electrodes to improve the electrical contact. In any case, the pass of

electricity was poor in some electrodes and the location of some profiles was moved. Therefore it is preferable to work in humid seasons when the terrain has this composition. Due to the proximity of the cliff, the Wenner-Schlumberger array has been selected for the data acquisition. In this condition, arrays like Dipole-Dipole tend to distort the measures. The data inversion has been performed with RES2DINV program. Additionally to the resistivity imaging, gypsum samples have been collected from different levels of the quarry in order to characterize them mineralogically, by means of analyzing the different mineral phases.

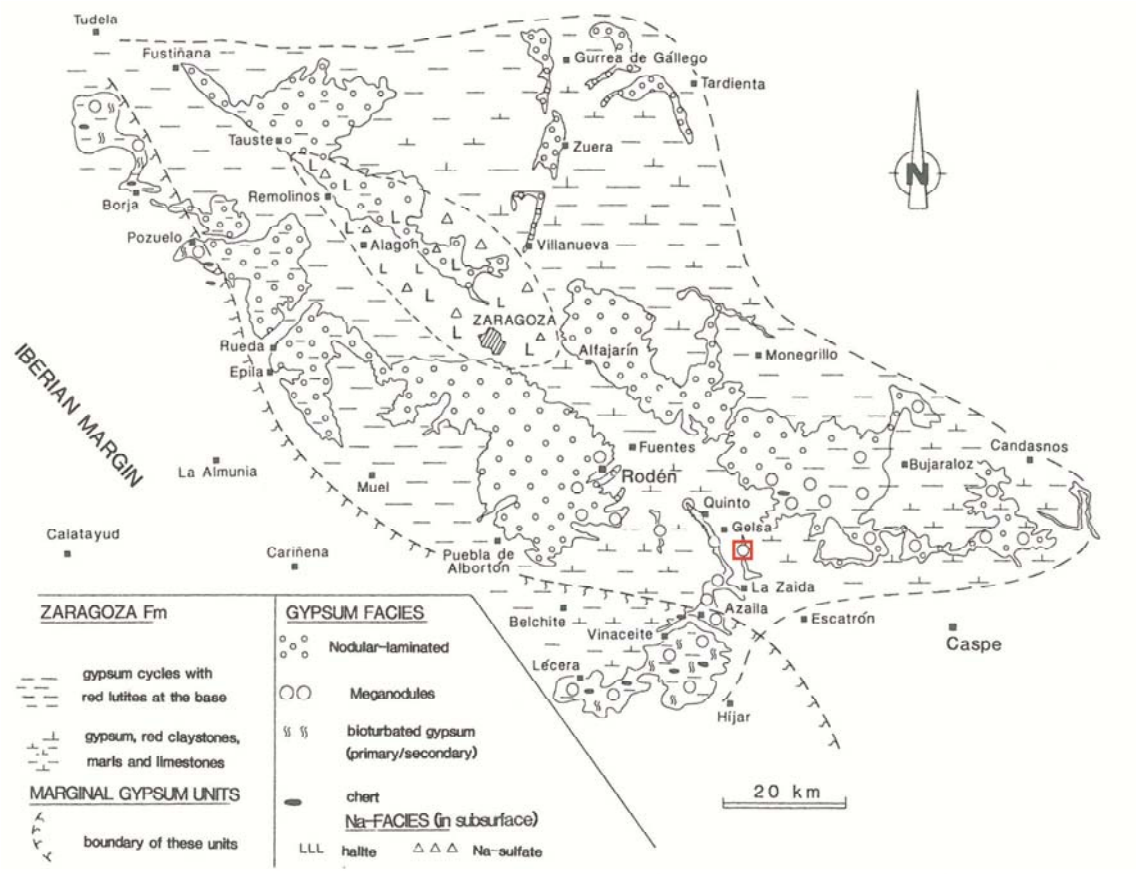

Figure 6.9: Geological map of the Central evaporitic Systems of the Ebro Basin. The studied area is marked with a red square (modified from Ortí and Salvany 1997).

.2.3 Geological setting and quarried gypsum unit

At the beginning of the Miocene, the subsidence in the Aragon sector of the actual Ebro basin increased, resulting in an important evaporitic deposition event. This evaporitic basin has a NW-SE disposition (figure 6.9) with approximately 80 km long and 40 km wide. The

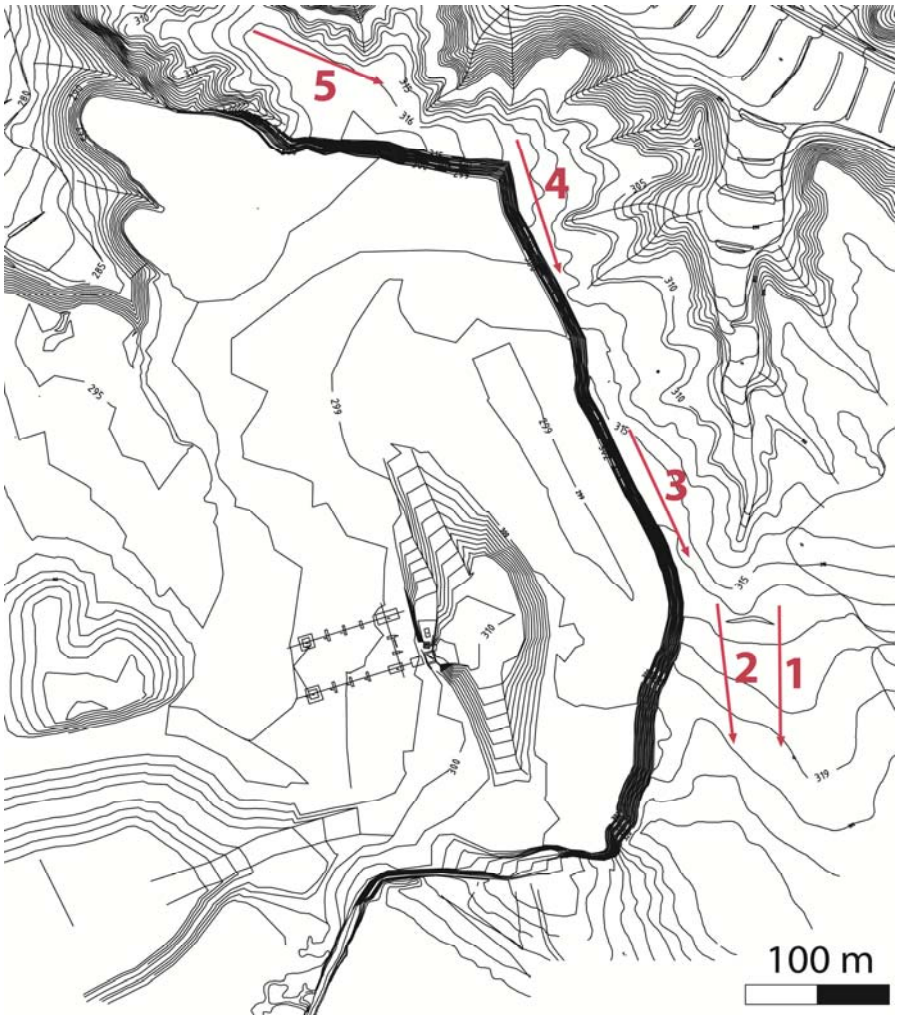

Figure 6.10: Topographic map of the active gypsum-quarry of Gelsa at the time of the survey (the quarry front changes as extraction process progresses). The location of the performed ERT profiles is marked with the red arrows.

outcropping evaporite units have a thickness of up to 100 meter (Ortí and Salvany 1997). In this basin, all sort of evaporitical phases were deposited in primary conditions (anhydrite, glauberite, halite…), but gypsum was predominant. This gypsum was transformed into secondary anhydrite and glauberite in early diagenesis. Nowadays this sequence is found in surface as secondary microcrystalline gypsum coming from the hydration of the anhydrous phases. The precipitation of these evaporitic sequences occurs in lacustrine or sabkha environments. Texturally, they are characterized by microcristalline gypsum, micro-macronodular alabastrine gypsum and chert.

The studied unit of Gelsa Gypsum is a peripheral lacustrine desposit of the sodic basin of Zaragoza, in which there is not sodium phases. There, nodular and laminated facies were

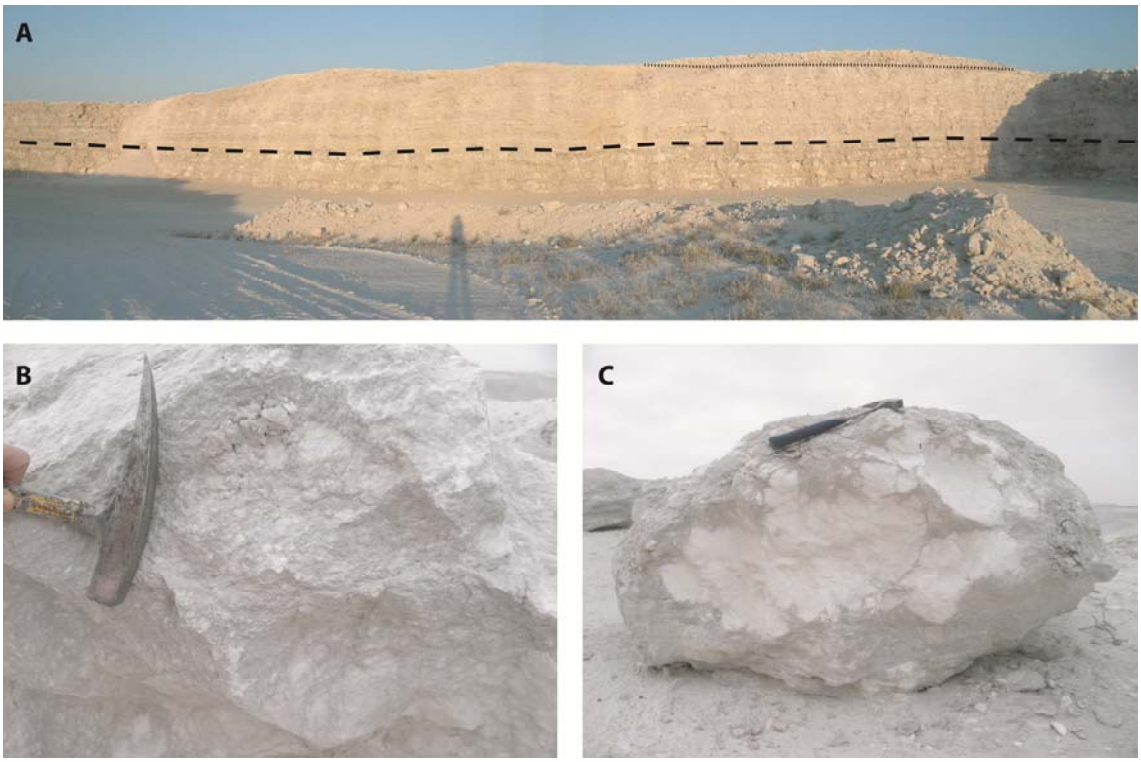

Figure 6.11: Photographs of the gypsum-quarry of Gelsa. A) General view of the quarry front, the dashed line indicates the transition between massive to layered (top) and alabastrine (bottom) gypsum subunits; the uppermost part is also composed of pure alabastrine gypsum (dotted line); B) Micronodular alabastrine gypsum in detail; C) Macronodular gypsum in a block in the upper SSE part of the quarry.

deposited. In the fronts of the quarry, it can be observed the composition of the different gypsum layers which outcrop and are being extracted (figure 6.11A). In general, the structure is horizontally layered. From base to top there is an alabastrine level (figure 6.11B) with macronodules. Above this level, there is a layered sequence of microcrystalline gypsum of approximately 5-7 meter (depending on the zone) with a thin (centrimetric) carbonate-lutite layer between the two different gypsum types. In the uppermost part there is an unconsolidated layer made of powdered gypsum (formed in the exploitation process and carried by the wind) and other lutitic materials of the surrounding terrain. The SSE part of the quarry front, where profiles 1 and 2 have been performed (figure 6.10), is topographically higher than the NNW part (few meters). In this part, another macronodular alabastrine layer can be observed above the layered gypsum level (figure 6.11A). Besides, there are some blocks in the upper part in which these macronodules can be identified (figure 6.11C). The purity in gypsum of the alabastrine macronodular layers is higher than the one of the layered gypsum one; up to 98% in purity in its purest parts compared with close to 90% of the latter one. In the current front there are not, but sometimes less pure metric bodies are found, making the

processing of the mineral less productive. Once the material of the current front is over, the extraction works will move towards the SE part of the area (figure 6.10).

.2.4 Results and discussion

Five ERT profiles have been performed in the gypsum quarry of Gelsa (Zaragoza). Profile 1 is located in the SSE part of the quarry while profiles 2 to 5 are situated along the quarry front (figure 6.10). In the inverted profiles, the RMS error between the calculated and measured pseudosection is lower than 5% in all cases. As the disposition of the gypsum layers of the deposit is horizontal, a similar trend is observed in all profiles, but with certain differences. In general we can identify 3 different layers (figure 6.12). The uppermost layer is a high resistivity one which corresponds with the unconsolidated dry terrain of the quarry. This layer is discontinuous and with variable thickness, but in general it has no more than 1 or 2 meters. Below the terrain level, a lower resistivity layer appears with a mean thickness of approximately 5 meters. This layer corresponds with the laminated secondary gypsum observed in the quarry front. At a depth of 5-7 meters, the electrical resistivity increases, corresponding to the lower alabastrine macronodular gypsum subunit. Below the gypsum deposit there is a Miocene clay unit, but this layer is not well shown because it is located at the bottom part of the profiles, where the sensitivity is lower. In any case, in all the profiles with the exception of profile 3, the resistivity tends to decrease at the lower part; this is well shown in the profiles 2 and 5.

The boundary between the nodular and massive to layered gypsum is curved in profiles 1, 2 and 4 (figures 6.12A, B and D) and more or less straight in profiles 3 and 5 (figures 6.12C and D); this is marked on the profiles by means of black dashed lines. In the case of profile 1, which is the one performed out of the quarry front, this boundary is particularly irregular and the nodular gypsum seems to be closer to the surface at some points. Moreover, between the 64 and 70 meters of the profile 1, there is not any resistive layer below the layered gypsum; which is present in the rest of the profile. This means that in that position, there is no pure nodular layer at depth. In the rest of the profiles, these sorts of discontinuities are not shown. As the future development of the quarry will spread towards that area, this decrease in the purity should be taken into account. The upper nodular level is observed in profile 5, this level is not shown in the quarry front, but in the ground in which the profile was performed (some meters above the top of the front) some pure gypsum outcrops can be

observed. This disposition has been confirmed by the quarry operators from the advances in the exploitation in that area. Therefore, it is showed that this upper alabastrine-nodular layer is present in both north and south of the deposit. In the south part the level only has been observed in the surface, but not in the terrain where the profiles have been performed (topographically below the top of the quarry front).

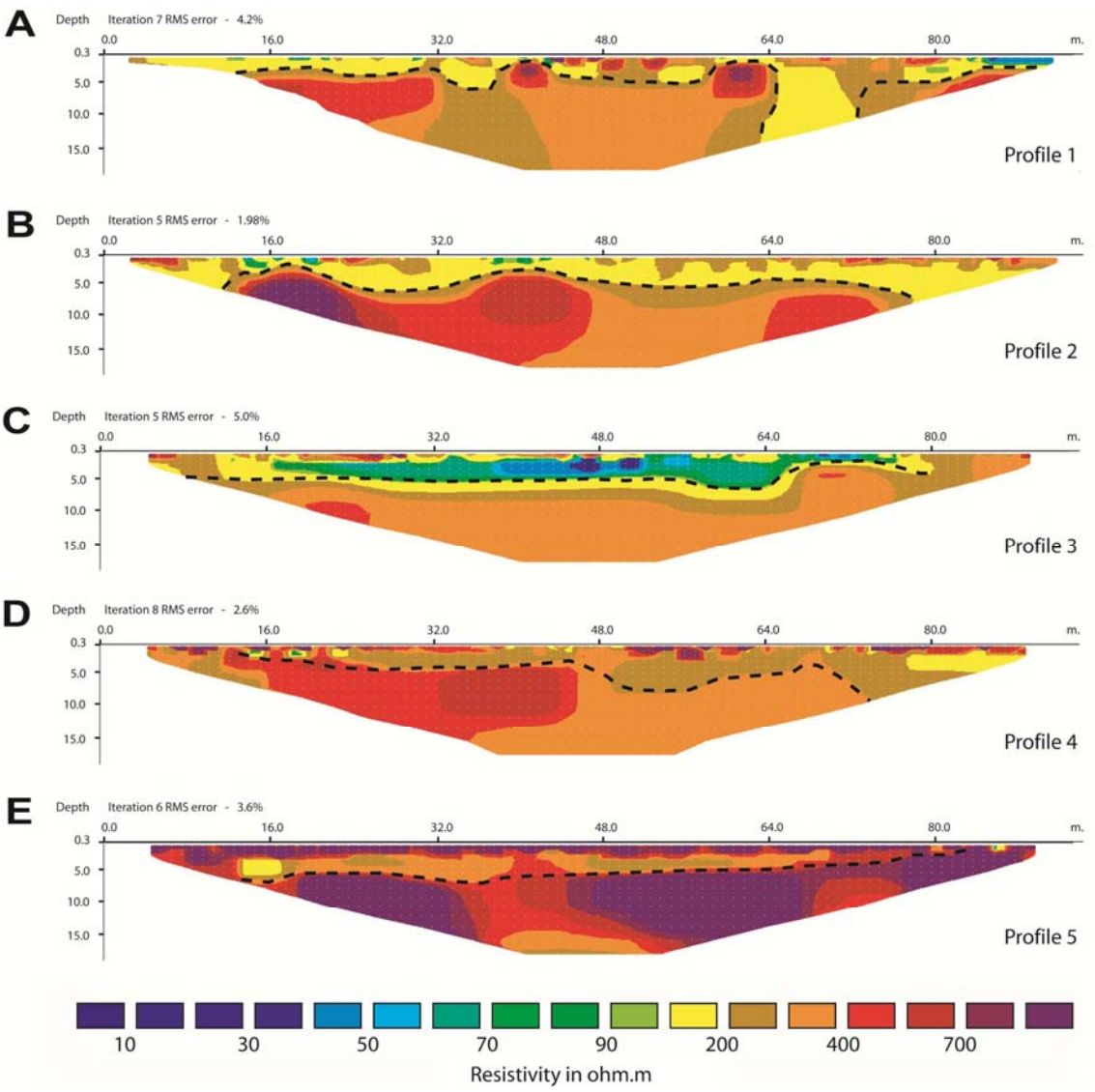

Figure 6.12: Inverted resistivity sections of gypsum quarry of Gelsa; the dashed line indicates the interpreted boundary between the massive to layered and alabastrine gypsum subunits. The situation of the profiles is showed in figure 6.10.

Respecting the resistivity values for the different gypsum levels, they should be considered as “Pure Gypsum” in the geoelectrical classification of gypsum rocks for all cases,

considering their purity and composition. For that type of gypsum rocks, a resistivity larger than 700 ohm.m is expected. In the present case, the calculated values are slightly lower in the case of some profiles. This is due to the inversion process and some effect of the clay which is below the whole deposit. In general, the apparent resistivity is larger than 400 ohm.m for deep measures, and in the case of profile 5 larger than 800 ohm.m; which should correspond to the expected values. In any case the calculated values are above the impure gypsum ones, which are below 100 ohm.m.

From the information obtained with the electrical imaging and the observations made in the front of the quarry, it is possible to determine the depth and the relative continuity of the nodular alabastrine gypsum layer, as well as the layered gypsum which is placed above. In the case of the layered gypsum, it is shown that the resistivity is lower in the southern profiles than in the northern ones; which should mean that the purity is larger in the layered gypsum of the north part of the quarry. The extraction works until now have shown this same trend, fitting with this observation. The exploitation works are made by steps, so to optimize the latter processing of the material, the first step should take the first 5-7 meters of the top gypsum layers (depending on the area), and afterwards remove the nodular gypsum which is below. With this planning, the obtained gypsum would have a more constant purity than if they are extracted both gypsum layers at the same time.